

**VALIDATION OF MARTIAN IMPACT CRATER GEOMETRY MEASUREMENTS.** S. T. Stewart, G. J. Valiant. Harvard University (Department of Earth and Planetary Sciences, 20 Oxford St., Cambridge, MA 02138, [sstewart@eps.harvard.edu](mailto:sstewart@eps.harvard.edu), [valiant@fas.harvard.edu](mailto:valiant@fas.harvard.edu)).

**Introduction.** Impact craters are a natural probe of planetary sub-surfaces. On Mars, crater excavation has launched meteorites and exposed sedimentary rock layers in crater walls. In addition, crater geometries seem to reflect the material properties of the target surfaces, showing regional and temporal variations [e.g., 1, 2].

Using the high resolution global topography data from Mars, quantitative measurements of impact crater geometries may be compared to numerical simulations in order to infer subsurface composition information, test rampart morphology formation hypotheses, or derive regional variations in surface properties. However, to be able to draw firm conclusions from crater geometry measurements, the measurement techniques must be validated and the measurement accuracy must be determined.

We have developed and tested a toolkit for measurements of crater geometry using the Mars Orbiter Laser Altimeter (MOLA) data. Here, we present a strategy for determining the accuracy of crater geometry measurements using simulated craters on ideal and actual background terrain. The validated measurement techniques are used to measure fresh impact craters from two highland and two lowland plains: Lunae Planum, Solis Planum, Utopia Planitia, and Isidis Planum.

**Crater Measurements Toolkit.** The features of the toolkit include:

(1) *Digital Elevation Maps (DEMs)*: Interactive generation of DEMs from MOLA PEDR altimetry profiles (tracks) at arbitrary spatial resolution for the region of interest. Data are gridded using the Delaunay triangulation (TRIGRID function in the IDL software package). Individual outlier altimetry tracks may be removed interactively, with recalculation of the DEM.

(2) *Crater rim*: Refinement of the user-estimated crater center by convolving a ring with the topography gradient; Calculation of crater radius, rim uplift height and their variances by interpolating the rim location along individual tracks that pass within a specified fraction (e.g., 0.8) of the estimated crater radius.

(3) *Background surface*: Definition of a background, pre-existing surface from user-specified tie points and the Delaunay triangulation across the crater cavity and ejecta blanket; Fitting of an exponential uplift profile, derived from cratering simulations, from the background to the crater rim.

(4) *Volumes*: Calculation of the crater cavity, ejecta blanket, and combined uplifted background and ejecta

volumes; Restriction of calculations to one or more pie-shaped wedges to avoid gaps in the altimetry data coverage and background topographic features (e.g., ridges, nearby craters, etc.) and/or calculations on user-specified regions drawn around the ejecta blanket (e.g., the inner vs. outer ejecta layer).

(5) *Visualization*: Generation of 2-D shaded relief views and 3-D shaded surfaces of the DEM, background surface, and ejecta blankets; Viewing of track coverage, along-track profiles or arbitrary profiles through the DEM; Comparison of the generated DEM to the MOLA DEMs distributed through the Planetary Data System; Viewing of the Viking Orbiter Digital Image Maps for the region of interest.

(6) *Logs*: Record of interactive measurements which may be run again (e.g., to compare different fitting algorithms) and a crater measurement output file.

**Resolution and Measurement Validation using Simulated Crater Sets.** We tested our toolkit for systematic errors and resolution sensitivity using simulated craters on different background surfaces, sampled at three different synthetic altimetry track densities (representative of the MOLA coverage at the equator, mid-, and high-latitudes) to generate synthetic DEMs using the same interpolation scheme as used on the MOLA data (Fig. 1). We considered an ideal flat background and three backgrounds generated by tiling patches from Mars with few large craters, centered at (i) 33°N, 200°E (Arcadia Pl.), (ii) 7°N, 290°E (Lunae Pl.), and (iii) 32°N, 98°E (Utopia Pl.).

The simulated crater sets, composed of 15 craters each in 8 size bins between 2 and 50 km rim diameter ( $D_R$ ), included randomly generated ejecta blanket profiles (within a realistic parameter range), with both single and double-layered rampart ejecta blankets. Identical measurements were performed on each background and at each track density at a DEM resolution of 0.3 km/pix for  $D_R \geq 6$  km and 0.15 km/pix for  $D_R \leq 4$  km.

Overall, the MOLA data resolves craters with  $D_R \geq 6$  km at all latitudes (Figs. 1C, 2B). Measurement accuracy begins to degrade when the number of points around the rim falls below about 10, although reasonable measurements are possible with as few as 4 rim points on  $D_R = 4$  km craters. Large-scale topographic features that cannot be interpolated in the background surface provide the greatest source of error on volume measurements of craters with  $D_R > 20$  km.

**Resolved Differences between Crater Geometries in Highland and Lowland Terrains.** We present the results from a survey of crater geometries in Utopia Planitia (U.P.) (area limited to [30-60°N, 105-124°E]), Isidis Planum (I.P.) [5-19°N, 75-105°E], Lunae Planum (L.P.) [6-20°N, 286-302°E], and Solis Planum (S.P.) [15-30°S, 260-285°E]. We measured all fresh craters with  $D_R > 4$  km that contained 4 or more track points on the rim. Fresh craters were identified by their depth to diameter ratio and ejecta blanket preservation (Fig. 4). The pie-wedge tool was used to omit gaps in track coverage and the ridges in L.P. In these cases, calculated volumes are corrected for the missing section assuming cylindrical symmetry. Our final set contained 54 craters ( $3.9 < D_R < 44.2$  km) in L.P., 45 craters in S.P. ( $2.0 < D_R < 37.0$  km), 16 crater in I.P. ( $4.3 < D_R < 47.7$  km), and 20 craters ( $5.6 < D_R < 46$  km) in U.P.

We find large, resolved differences between regions in rim uplift height (Fig. 2), ejecta volume (Fig. 3), crater depth (Fig. 4), and crater cavity volume. For a given diameter, the craters in the lowland plains are deeper, have higher rims, and larger ejecta blankets. The observed variations are generally 2 to 5 times greater than the standard deviation ( $\sigma$ ) in measurement errors derived from the simulated crater tests. Although ejecta volumes around the smallest craters in Lunae Planum and Solis Planum are comparable to the absolute errors in the simulated craters, the simulations confirm that there is little systematic offset on any of the background terrains. For example, Fig. 3A shows excellent correlation between craters within each region of study. Hence, we have confidence in the statistical significant and overall accuracy of the measurements in the four study regions.

**Validation between Research Groups.** We propose that impact crater measurement techniques be validated using a standard set of simulated craters. In addition to using simulated craters as a benchmark for measurement accuracies, we also propose direct comparisons between different methods for background (pre-impact) surface subtraction and ejecta volume calculations.

The simulated craters used in this study are available on the web at: <http://www.shock.eps.harvard.edu>. The crater sets are distributed as IDL (www.rsinc.com) ‘save’ files, composed of simulated tracks (latitude, longitude) at 3 different track densities, simulated altitudes (for each crater size, track density, and background), and simulated crater DEMs on a flat background. The input geometric parameters for each simulated crater are tabulated for comparison to measurements.

This set of simulated fresh craters does not encompass all of the challenges encountered in crater measurements, e.g., degraded and severely non-axisymmetric craters. We find that tailored simulated crater sets should be generated to gauge the accuracy of measurements of specific types of craters on representative background terrains.

**Conclusions.** Simulated crater sets provide confidence and absolute accuracy estimates for crater geometry measurements using the MOLA global topography. Simulated craters must be tailored for the type of crater forms and background terrain. This validation technique has been applied to fresh craters on highland and lowland terrains, where significant differences ( $2-5 \sigma$ ) are resolved with confidence. We propose that research groups measuring crater forms adopt a standard suite of simulated craters to benchmark the accuracy of different measurement methods.

**Acknowledgements.** This work is supported by NASA MDAP under contract NAG5-13474.

#### References.

- [1] Barlow, N.G. and T.L. Bradley (1990) *Icarus* **87**, 156-179.
- [2] Valiant, G.J. and S.T. Stewart (2004) *Proc. Lunar & Planetary Science Conference* **34**, Abstract #1293.
- [3] Garvin, J.B., et al. (2002) *Proc. Lunar & Planetary Science Conference* **33**, Abstract #1255.
- [4] Pike, R.J. (1980) *Icarus* **43**(1), 1-19.

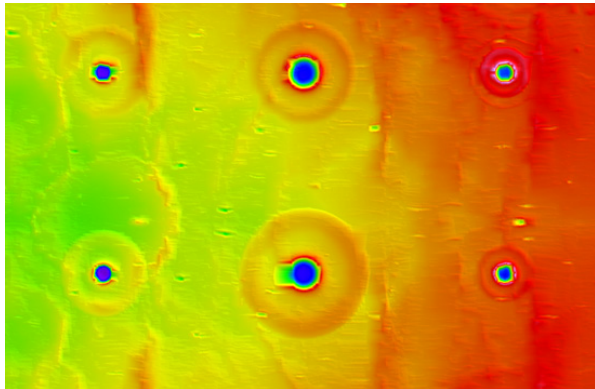


**Fig. 1.** Example field of simulated craters on terrain model based on Lunae Planum.

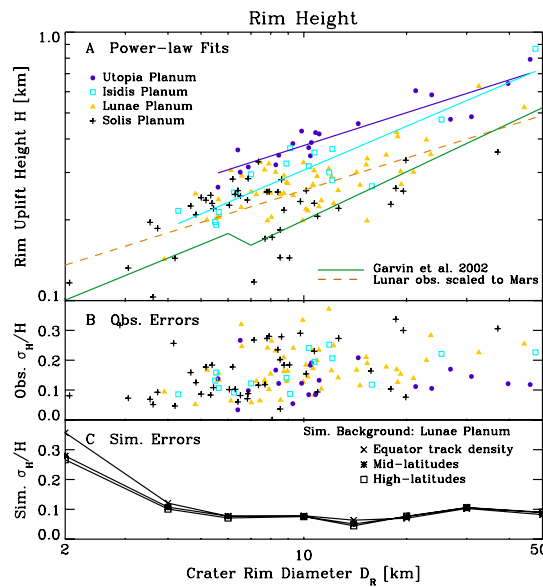


**Fig. 2.** **A.** Crater rim uplift heights above pre-impact surface with power law fits for each terrain. The global average [3] and scaled lunar data [4] are also shown. **B.** Fractional scatter in rim height measurements. **C.** Fractional measurement error on simulated craters.

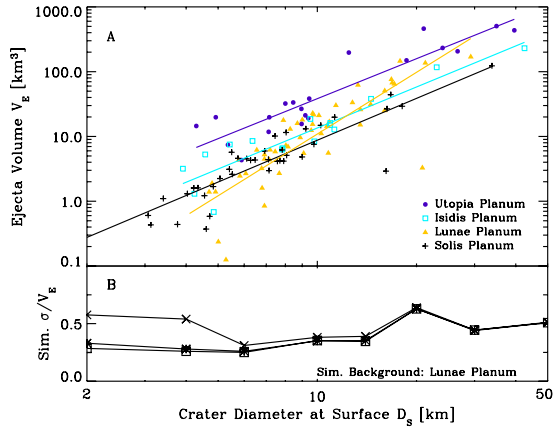


**Fig. 3.** **A.** Crater ejecta volume measurements with power law fits in each terrain. **B.** Fractional measurement error on simulated craters.

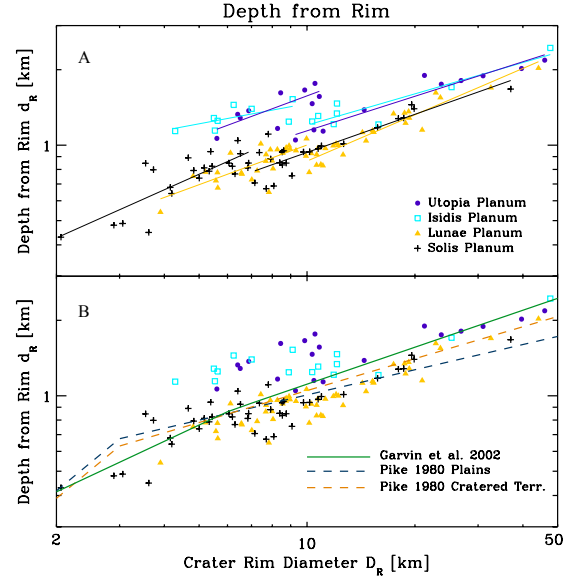


**Fig. 4.** Depth from rim vs. rim diameter with (A) power law fits in each terrain and (B) compared to global and regional averages [3, 4].